Received: 2 January 2020 | Revised: 24 April 2020 | Accepted: 6 July 2020
DOI: 10.1002/joc.6740

RESEARCH ARTICLE

International Journal of Climatology RMetS

Is it possible to fit extreme climate change indices together seamlessly in the era of accelerated warming?

Yizhak Yosef[1,2] | **Enric Aguilar**[3] | **Pinhas Alpert**[1]

[1]Department of Geophysics, Tel-Aviv University, Tel-Aviv, Israel
[2]Israel Meteorological Service, Bet-Dagan, Israel
[3]Center on Climate Change (C3), Rovira i Virgili University, Tarragona, Spain

Correspondence
Yizhak Yosef, Department of Geophysics, Tel-Aviv University, Tel-Aviv, Israel.
Email: yizhakyosef@mail.tau.ac.il

Abstract
This study examines the problematic impact of selecting a different base period (colder 1961–1990 vs. warmer 1988–2017), on the trend magnitude of widely used percentile-based extreme temperature indices (e.g., warm/cold spells, warm/cold days and nights). The percentile-based indices are part of a core set of indices (27 in total) that have become a common standard for monitoring climate change, as recommended by the Expert Team on Climate Change Detection and Indices (ETCCDI). The indices were designed to be comparable across regions provided that similar analyses are employed. Unfortunately, the use of different base periods and periods of interest to explore local and global climate change undermines the comparability of findings across regions. When utilizing "day-count" indices with fixed thresholds, the use of different base/reference periods changes the intercept without influencing the slope (for a given period length). However, this assertion does not hold with percentile-based indices. Our analyses show that percentile-based temperature indices (e.g., days with temperature below the 10th or above the 90th percentiles) are particularly susceptible to the problematic use of different base periods. Hence, using percentile-based indices may have adverse effects on researchers' conclusions. The current paper reports the results of a comparative study that used different base periods for the most commonly used percentile-based extreme temperature indices. It was found that the (negative) trend magnitude of the cold percentile-based indices (frequency of cold days and nights and cold spells) is strongly amplified while the (positive) trend magnitude of the warm indices (frequency of warm days and nights and warm spells) is dramatically diminished when percentiles were derived from a base period that included records from the last two decades (e.g., 1981–2010, 1988–2017). These features are even more pronounced when the study period covers only the last 30–40 years.

KEYWORDS
base period, climate change, climate extreme indices, percentile-based indices, warming trends

1 | INTRODUCTION

The past two decades witnessed a steady increase in the application of the Expert Team on Climate Change Detection and Indices (ETCCDI) recommendations for monitoring climate extremes (including by the Intergovernmental Panel on Climate Change, IPCC; e.g., Frich et al., 2002; Aguilar *et al*., 2005; Zhang *et al*., 2005a; Alexander *et al*., 2006; Klein Tank *et al*., 2006; Vincent and Mekis, 2006; Donat *et al*., 2013; Yosef *et al*., 2019). The ETCCDI defined a total core set of 27 indices based on daily temperature values or daily precipitation amount. Some indices are based on fixed thresholds for all stations (for instance, 25°C threshold as used in the summer days index [SU25] or days below 0°C threshold to indicate frost days [FD0]). In contrast, other indices are based on thresholds that vary from location to location. In these cases, thresholds are typically defined as a percentile of the relevant data series. The ETCCDI day-count indices that based on percentile thresholds are chosen so that they will be exceeded at a fixed frequency, often 10%, during the base period that is used to define the thresholds. This refers to moderate extremes and climate extremes with short return periods that typically occur several times every year (Klein Tank *et al*., 2009; Zhang *et al*., 2011). Since changes in percentile-based indices do not necessarily translate to changes in absolute extremes (Zhang *et al*., 2001), for rare extreme events that lie far in the tails of the probability distribution, the two general approaches: block-maxima and peak-over-threshold (POT), are more suitable. The block-maxima method requires a sample of extreme values obtained by selecting the maximum (or the minimum) value observed in each block. Blocks are typically annual (365 daily observations per block) or seasonal. This can be modelled with generalized extreme value (GEV) distribution. The POT approach considers all sample values that exceed a high, predefined threshold. The probability distribution of the exceedances over the threshold can be modelled using the generalized Pareto distribution (GPD).

The rationale underlying the introduction of the ETCCDI core set of indices was to enable individuals, countries, and regions to calculate the indices in exactly the same way such that their analyses will fit seamlessly into the global picture (Karl *et al*., 1999; Peterson *et al*., 2001). The indices were published in the World Meteorological Organization (WMO) guidelines on the analysis of extremes in a changing climate by Klein Tank *et al*. (2009) and by Zhang *et al*. (2011), who applied a bootstrapping procedure to determine climatological percentile thresholds as a means to avoid discontinuities in the indices time series at the beginning or end of the base period (Zhang *et al*., 2005b).

Recently, Salameh *et al*. (2019) published a study of the changes in climate extreme indices (utilizing the ETCCDI indices) across Israel in the period 1987–2016. Their database was homogenized by using absolute homogenization methods. Yosef *et al*. (2019), who similarly studied changes in climate extreme indices across Israel, had analysed a longer period 1950–2017, compared it to the 1988–2017 period, and applied a more robust homogenization procedure using relative homogenization methods in conjunction with metadata. A comparison of the spatial and the averaged regional trends of the percentile-based indices (e.g., warm/cold spells duration, warm/cold days and nights) in the two studies (i.e., Salameh *et al*., 2019; Yosef *et al*., 2019) reveals different results that cannot be attributed to the use of different homogenization methods. For instance, Yosef *et al*. (2019) reported a significant increasing trend of 8.03 days per decade in the WSDI (warm spell duration index) over the period 1988–2017, whereas Salameh *et al*. (2019) reported a much smaller increase of only 0.63 days per decade over the nearly identical period of 1987–2016. Since both studies used similar weather stations and almost the same period of interest, this large discrepancy should be attributed mainly to the selected base period. Whereas Yosef *et al*. (2019) derived the percentiles from the standard normal base period 1961–1990, Salameh *et al*. (2019) used 1987–2016 as their base period.

Previous studies that applied percentile-based indices have generally overlooked the problematic impact of the tendency to use different base periods across different studies. Here, we highlight the negative impact of heterogeneity in the selection of base periods. Specifically, we demonstrate how the selection of different base periods can result in misleading conclusions when using percentile-based extreme temperature indices.

2 | METHODOLOGY

2.1 | Database

The database contains 24 long-term station records from various climatic regions across Israel. All the maximum temperature (TX) and the minimum temperature (TN) time series have undergone a quality control and a thorough relative homogenization routine following the procedures employed by Yosef *et al*. (2019). We applied state-of-the-art homogenization methods (e.g., HOMER, ACMANT, CLIMATOL), taking into account metadata (the historical information about the stations) in order to validate the results (i.e., break-points detection). Missing daily values of the adjusted database were completed by linear regression based on highly correlated stations. Information about the stations' coordinates, heights and periods of homogenous data appear in Table 1.

2.2 | Percentile-based extreme indices

The ETCCDI were actively coordinated by the Climate Variability and Predictability (CLIVAR)/Commission for Climatology (CCl)/Joint Technical Commission for Oceanography and Marine Meteorology (JCOMM). Additionally, the WMO Commission for Climatology established an Expert Team on Sector-specific Climate Indices (ET-SCI), which consider agriculture, water, and health sectors requirements alongside the ETCCDI indices (Alexander and Herold, 2015). In order to calculate these extreme indices derived from daily data, we employed a specially developed "R" software package ClimPACTv2 package (Alexander and Herold, 2015), for both ETCCDI and ET-SCI indices. This package includes Zhang *et al.*'s (2005b) bootstrapping procedure.

As mentioned above, these climate extreme indices are calculated based on daily observed minimum and maximum temperatures or daily precipitation amount. Some indices involve counting the number of days (in a season or a year) that exceed specific thresholds defined as percentiles; thus, their thresholds change from one site to another. While the 95th and 99th percentiles of precipitation on wet days are fixed thresholds in a given base period n, the temperature percentile-based indices have an annual cycle (i.e., for the same percentile each calendar day has a different calculated threshold in a base period n). The percentile-based thresholds of the temperature base period were calculated from five-day windows centered on each calendar day. When necessary, days from adjacent years are taken (i.e., January first is represented by December 30th, 31st, 1st, 2nd and 3rd) to account for the mean annual cycle. A five-day window is chosen to yield a total sample size of 30 years (the base period length) × 5 days = 150 (days) for each calendar day, which results in a relatively smooth annual cycle of percentile thresholds. This procedure, defined by the

TABLE 1 List of weather stations and their periods of homogeneous data

Station name	Latitude	Longitude	Altitude (m)	Period
Dafna	33.22	35.63	135	1950–2017
Kefar-Blum	33.17	35.60	75	1950–2017
Zefat (Har-Kenaan)	32.97	35.50	936	1950–2017
Akko	32.93	35.10	8	1950–2017
Bet-Zayda	32.87	35.65	−200	1950–2017
Tavor (Kadoorie)	32.70	35.40	145	1950–2017
Zemah	32.72	35.58	−200	1950–2017
Kefar-Yehoshua	32.68	35.15	50	1950–2017
Afula	32.60	35.27	60	1950–2017
Galed	32.55	35.07	180	1950–2017
Sede-Eliyyahu	32.43	35.50	−185	1950–2017
En-Hahoresh	32.38	34.93	15	1950–2017
Tel-Aviv (coast)	32.05	34.75	10	1950–2017
Bet-Dagan	32.00	34.80	31	1950–2017
Qevuzat-Yavne	31.82	34.72	50	1950–2017
Jerusalem (center)	31.77	35.22	810	1950–2017
Beit-Jimal	31.72	34.98	355	1950–2017
Negba	31.65	34.67	95	1950–2017
Dorot	31.50	34.63	115	1950–2017
Besor farm	31.27	34.38	110	1950–2017
Beer-Sheva	31.25	34.80	279	1950–2017
Sedom	31.02	35.38	−388	1950–2017
Sede-Boqer	30.87	34.78	475	1950–2017
Elat	29.55	34.95	22	1950–2017

ETCCDI, ensures that extreme temperature events, in terms of crossings percentile thresholds, can occur with equal probability throughout the year (Klein Tank *et al.*, 2009).

The percentiles of the current study were derived from two different base periods for comparison. The first base period was the standard normal period 1961–1990 (WMO, 2017). The second base period was 1988–2017. The first base period captures a relatively cold period whereas the second base period captures a much warmer period.

The selected percentile-based indices were: WSDI and WSDI3 (warm spell duration index with at least 6 or 3 consecutive days when TX > 90th percentile, respectively), CSDI3 (cold spell with at least 3 consecutive days when TN < 10th percentile), TX10p (cold days), TX90p (warm days), TN10 (cold nights) and TN90p (warm nights). Table 2 presents a list of these indices with their acronyms and short definitions. The CSDI3 index (based on 3 days sequences) was chosen rather than the more common CSDI (based on 6 days sequences) since the latter is very rare in the Israeli region and as consequence its statistics are less robust.

2.3 | Area average

To summarize the long-term changes observed in Israel (1950–2017), regional averages for every index were computed. The regional averaged temperature indices were computed as an unweighted mean of the indices at individual stations relative to their climatological averages. This was done twice, once with the percentiles derived from the colder base period 1961–1990 and a second time with the percentiles derived from the warmer base period 1988–2017. The anomalies in this study were calculated relative to 1961–1990 mean values.

2.4 | Trend calculations

Trends for the various indices time series were calculated for different periods of interest since 1950, focusing on the recent 30 years, that is, 1988–2017. The robust non-parametric Mann-Kendall test (Mann, 1945; Kendall, 1955) with Sen's slope estimator (Sen, 1968) was applied to the time series, since it is not affected by the distribution of the data, nor is it sensitive to outliers. All the time series were pre-whitened in order to correct the Mann-Kendall test for serial autocorrelation (Zhang *et al.*, 2000; Wang and Swail, 2001). We consider a trend to be significant if it is statistically significant at the 5% level. This trend analysis was conducted using the R package "zyp" (Bronaugh and Werner, 2013).

3 | RESULTS

Figure 1 shows the changes in the percentile thresholds when they are derived from the two base periods, 1961–1990 (colder) versus 1988–2017 (warmer). The analysis was done for Jerusalem and Bet-Dagan stations, which are located in different climatic zones. Jerusalem is located inland in a mountainous region (altitude 815 m), whereas Bet-Dagan is located in the coastal plain (altitude 33 m). It can be noticed that the daily thresholds for the recent period (1988–2017) are much warmer than in the past (1961–1990) for both the 10th and 90th percentiles. The differences between the two base periods were calculated by subtracting the threshold of each day of the

TABLE 2 Percentile-based extreme indices recommended by the expert teams (ET)

Index	Indicator name	Definitions	ET	Unit
TX10p	Cool days	Percentage of days when TX < 10th percentile	ETCCDI	%
TX90p	Warm days	Percentage of days when TX > 90th percentile	ETCCDI	%
TN10p	Cool nights	Percentage of days when TN < 10th percentile	ETCCDI	%
TN90p	Warm nights	Percentage of days when TN > 90th percentile	ETCCDI	%
WSDI	Warm spell duration indicator	Annual count of days with at least 6 consecutive days when TX > 90th percentile	ETCCDI	Days
WSDI3	Warm spell duration indicator	Annual count of days with at least 3 consecutive days when TX > 90th percentile	ET-SCI	Days
CSDI	Cold spell duration indicator	Annual count of days with at least 6 consecutive days when TN < 10th percentile	ETCCDI	Days
CSDI3	Cold spell duration indicator	Annual count of days with at least 3 consecutive days when TN < 10th percentile	ET-SCI	Days

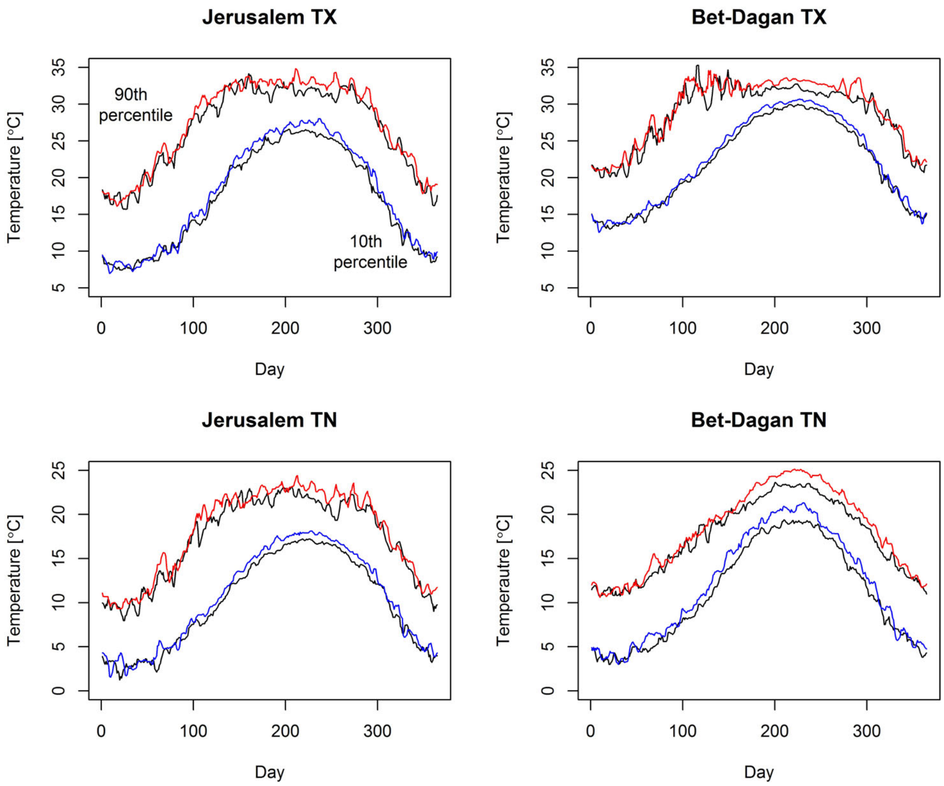

FIGURE 1 The percentile-based thresholds of the maximum (TX) and minimum (TN) temperature, derived from two base periods, 1961–1990 (black) and 1988–2017 (red and blue). In each panel, the upper curves denote the 90th percentile and the lower curves denote the 10th percentiles. The thresholds for Jerusalem and bet-Dagan stations appear on the left and right panels, respectively [Colour figure can be viewed at wileyonlinelibrary.com]

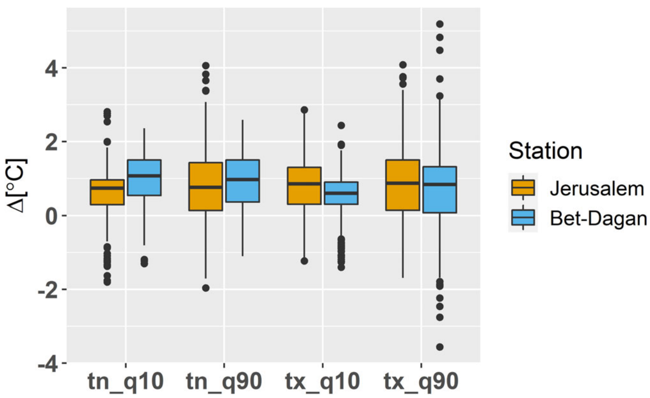

FIGURE 2 The distribution of the differences when subtracting the threshold of each day in the warm period 1988–2017 from the cooler period 1961–1990, at the 10th and the 90th percentiles. Jerusalem appears in orange and bet-Dagan appears in blue [Colour figure can be viewed at wileyonlinelibrary.com]

warmer period 1988–2017 from the cooler period 1961–1990. The distributions of these differences are presented in Figure 2. Analysing these distributions revealed a similar positive deviation for both stations for the different thresholds (quantiles). The total average difference is ~0.8°C for each station. The averaged interquartile ranges (IQR) are also similar and equal to 0.99°C and 1.09°C at Bet-Dagan and Jerusalem, respectively. Moreover, the deviations fluctuated (i.e., they are non-constant) throughout the annual cycle for both thresholds (10th and 90th percentiles). The warmer months showed the largest deviations whereas the cold months (mainly November until February) exhibited smaller deviations. These large, fluctuating deviations for both TX and TN are noteworthy; they lead to higher thresholds in the later (1988–2017, warmer) period that the observations need to exceed to qualify as extreme, which ultimately may have an impact on the trends ratio.

Figure 3 presents the spatial and regional average trends of WSDI and CSDI3 indices. Here, the maps show only the trends for the last 30 years (1988–2017) when percentiles were derived from different base periods (b.period 1961–1990 and b.period 1988–2017). For exactly the same period of interest, a significant dissimilarity between the two analyses was found. For the WSDI, when percentiles were derived from the warmer base period (1988–2017), null spatial trends were detected. This is in contrast to the highly significant and substantial changes when a colder base period was used (1961–1990). The opposite pattern emerged with the CSDI3 trends: Whereas significant negative trends were found when the warmer base period was applied (1988–2017), only mild changes (mostly non-significant statistically) were found when a colder base period (1961–1990) was used.

The averaged regional time series anomalies (relative to 1961–1990), shown on the bottom of Figure 3, depict the long and short-term changes when different base

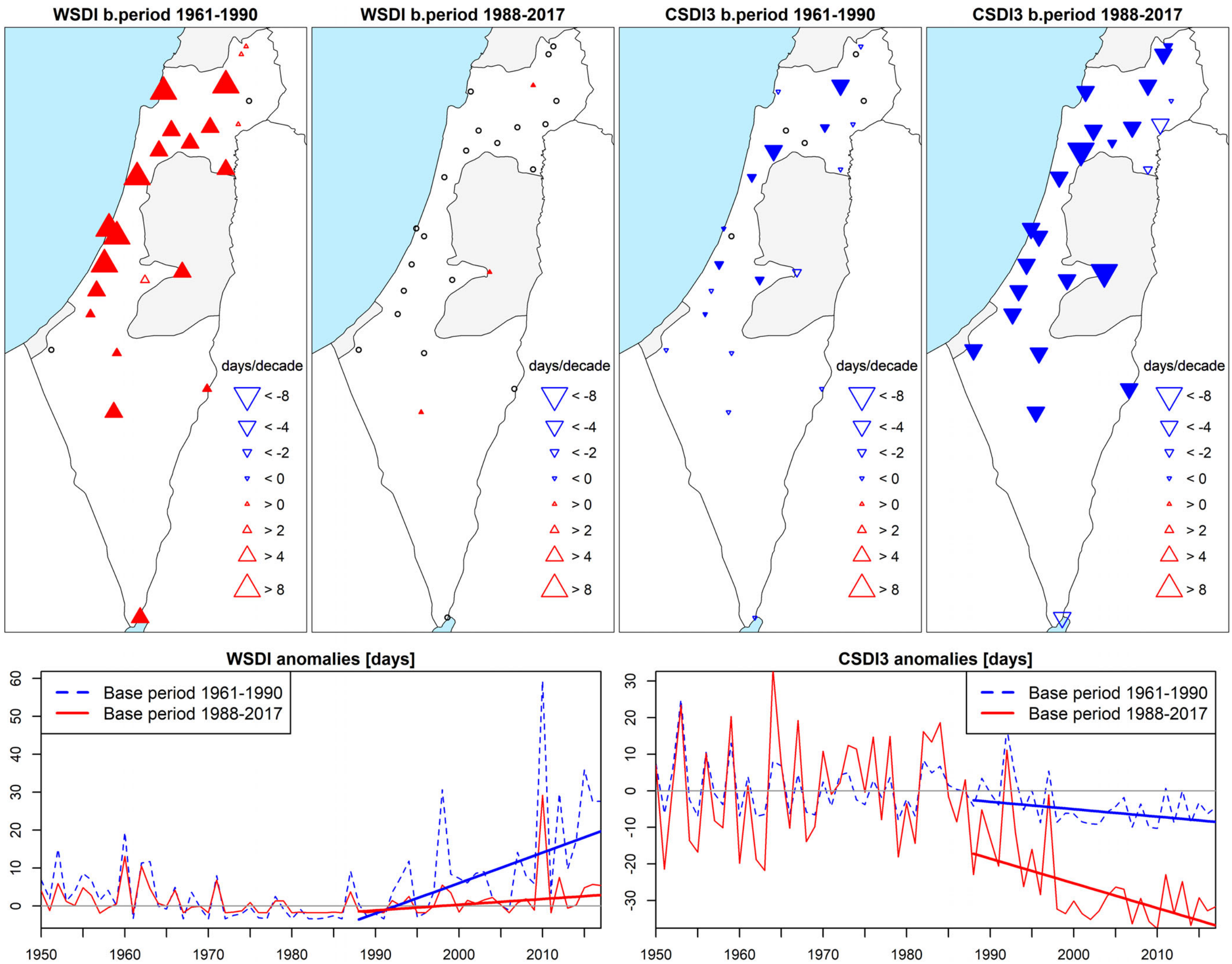

FIGURE 3 The maps display the trends in the WSDI and CSDI3 indices for the period 1988–2017 when percentiles derived from different base periods (b.period 1961–1990 vs. b.period 1988–2017). Upward facing red triangles represent increasing trends and downward facing blue triangles represent decreasing trends. Different sizes of triangles indicate different magnitudes of trends. Filled triangles mark significant changes ($p \leq .05$; units: days per decade). Circle denote no trend. The graphs display regional averaged anomaly series (1950–2017) relative to 1961–1990 mean values. Solid (red) and dashed (blue) lines represent the different base periods of which the percentiles were derived, 1988–2017 (warmer) and 1961–1990 (colder) respectively. Solid blue and red lines denote the linear trends of the period 1988–2017 for both base periods [Colour figure can be viewed at wileyonlinelibrary.com]

periods are used, for both indices. The warm index (WSDI), exhibits a sharp increase that starts at the beginning of the 1990s, whereas the cold index (CSDI3) exhibits a mild decrease at the same time (red lines). This is when the percentiles were derived from a colder base period, 1961–1990.

The opposite occurred when a warmer base period was used to derive the percentiles, which led to almost no change in the WSDI, and on the other hand, to a steep decrease in the trend of CSDI3 index (red lines, Figure 3, bottom right). The regional averaged WSDI trend for the period of interest 1988–2017 is 8.03 days per decade versus 1.5 days per decade when colder (1961–1990) and warmer (1988–2017) base periods were used, respectively (denoted by the linear trend lines in Figure 3, bottom left). Furthermore, the CSDI3 trends are three times lower, with −2.04 days per decade versus −6.76 days per decade, when colder versus warmer base periods were applied, respectively. For the WSDI3 index, which is more frequent in our region, the trends are three times higher in this period of interest with 14.92 days per decade (when colder base period, 1961–1990, was used) versus 4.59 days per decade (when warmer base period, 1988–2017, was used). Tables 3 and 4 summarize the annual and the seasonal trends over 1988–2017, using both base periods.

The same principle holds for the common percentile-based indices TX10p (cold days), TX90p (warm days), TN10p (cold nights) and TN90p (warm nights), which describe the left and the right tails of the temperature distribution. Figure 4 shows the four indices of long and short term trends for the annual regional averages anomalies (relative to 1961–1990). When a warmer base period was used (1988–2017), the cold indices (TX10p and TN10p) exhibited a strong decrease (around two times greater), whereas the warm indices (TX90p and TN90p) exhibited a mild increase (about two times smaller, Table 4). Additionally, large discrepancies emerged for all seasons except winter (Table 4). Table 5 shows the difference between the outcomes (i.e., the indices slopes calculated using the warmer base period minus the colder base period). The differences in the annual trends, for the warm as well as the cold indices, were found to be significant. These deviations are even more pronounced in the summer; this season was characterized by the largest significant dissimilarity as compared with the other seasons (Table 5).

Figure 5 illustrates this point by showing the spatial distribution trends on maps. The upper and the lower panels display the trends for the same period of interest (1988–2017). The upper panels present the trends when the colder base period was used whereas the lower panels show the trends when the warmer base period was applied. As in Figure 3, the trends in the upper and lower panels should in principle be the same regardless of the selected base period (e.g., in a day-count indices exceeding a certain fixed thresholds or as in absolute temperature anomalies). However, we found large discrepancies between the upper and the lower maps.

We subsequently calculated trend matrices to examine the effects of using different period lengths on percentile-based indices. Figure 6 displays the annual trends and their statistical significance ($p \le .05$, black "+") for all the possible combinations of starting (x-axis) and ending years (y-axis), with 30 or more years of observations. The diagonal displays trend results of a 30-year time period, beginning in the lower left corner with the period 1950–1979, progressing with one-year steps and ending in the upper right corner with the period 1988–2017. In the upper left corner the result of the entire series (1950–2017) can be found. The right column of Figure 6 shows the difference between the periods when percentiles were derived from 1988–2017 (warmer period, middle column) to percentiles that were derived from 1961–1990 (colder period, left column). As the beginning year (x-axis) is progressing towards current day, the magnitude of the negative difference between the trends obtained from the two inspected base periods is increasing (most pronounced for warm nights index, TN90p, Figure 6l). It is clear that the tendency towards amplifying or diminishing trends is a function of the chosen base period.

4 | DISCUSSION

The global temperature has been changing vigorously in the last 30 years. The Earth's surface temperature has been successively warmer than in any preceding decade since 1850 (Donat *et al.*, 2013; IPCC, 2014). Figures 1 and 2 clearly demonstrate these typical changes that occurred in the last three decades compared to the common standard normal base period 1961–1990. In addition, on a global scale, it is very likely that a decline in the number of cold days and nights has taken place, while the frequency of warm days and nights have increased. Moreover, heat waves have become more frequent in many parts of Europe, Asia and Australia (IPCC, 2014). To estimate these changes properly, the use of a relatively colder base period, such as 1961–1990, is needed.

Klein Tank *et al.* (2009) stipulated that the choice of another normal period (e.g., 1971–2000) has only a small impact on the results when estimating the changes in the indices over time. This assertion accords with Yosef *et al.* (2019), which showed that percentiles from the base period 1961–1990 and 1971–2000 have a similar impact on trend magnitude of order. However, this assertion does not hold in a rapidly changing (non-stationary climate) world that exhibits a clear and continued warming trend. The results of the current study indicate that the choice of a base period has a marked impact on the magnitude of the slope, especially when a warmer base period (e.g., 1981–2010, 1988–2017) is used. Specifically, it was

TABLE 3 Annual trends (days per decade) for the period 1988–2017, using two base periods, 1961–1990 and 1988–2017

	WSDI base period 1961–1990 [days per decade]	WSDI base period 1988–2017 [days per decade]	WSDI3 base period 1961–1990 [days per decade]	WSDI3 base period 1988–2017 [days per decade]	CSDI3 base period 1961–1990 [days per decade]	CSDI3 base period 1988–2017 [days per decade]
Annual	**8.03**	**1.5**	**14.92**	**4.59**	−2.04	**−6.76**

Note: Bold values denote statistical significance at the $p \le .05$ level.

TABLE 4 Annual and seasonal trends (% per decade) for the period 1988–2017, using two base periods, 1961–1990 and 1988–2017. The change in the annual number of the days per decade are displayed in parentheses (the seasonal percentages are quite similar to the actual number of days in a season)

	TX10p base period 1961–1990 (% per decade)	TX10p base period 1988–2017 (% per decade)	TX90p base period 1961–1990 (% per decade)	TX90p base period 1988–2017 (% per decade)	TN10p base period 1961–1990 (% per decade)	TN10p base period 1988–2017 (% per decade)	TN90p base period 1961–1990 (% per decade)	TN90p base period 1988–2017 (% per decade)
Spring	**−3.82**	**−5.43**	2.09	1.41	**−2.84**	**−5.68**	**2.76**	**2.00**
Summer	−1.38	**−6.28**	**10.41**	**5.12**	**−1.27**	**−7.55**	**14.55**	**5.67**
Autumn	**−2.65**	**−5.5**	2.00	0.2	**−2.00**	**−4.88**	**4.33**	1.4
Winter	−0.9	−1.04	**5.49**	**4.24**	−0.6	−0.77	**4.55**	**3.64**
Annual	**−2.36 (−9)**	**−4.58 (−17)**	**5.11 (19)**	**2.76 (10)**	**−1.77 (−6)**	**−4.76 (−17)**	**6.9 (25)**	**3.33 (12)**

Note: Bold values denote statistical significance at the $p \leq .05$ level.

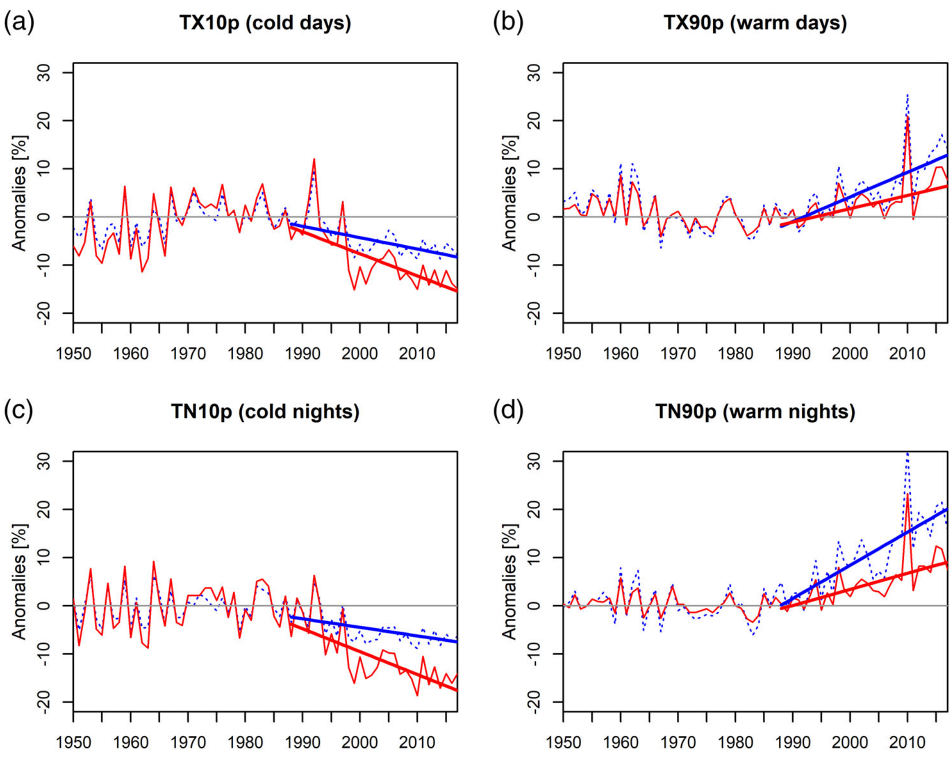

FIGURE 4 Regional averaged anomaly series (1950–2017) relative to 1961–1990 mean values of four percentile-based indices: TX10p, TX90p, TN10p, and TN90p. Solid (red) and dashed (blue) lines represent the two base periods from which the percentiles were derived, 1988–2017 (warmer) and 1961–1990 (colder) respectively. Solid blue and red lines denote the linear trends of the period 1988–2017 for both base periods [Colour figure can be viewed at wileyonlinelibrary.com]

TABLE 5 The difference in the trends magnitude per decade when selecting different base periods

	ΔWSDI	ΔWSDI3	ΔCSDI3	ΔTX10p	ΔTX90p	ΔTN10p	ΔTN90p
Spring	—	—	—	−1.61	−0.68	**−2.84**	−0.76
Summer	—	—	—	**−4.9**	**−5.29**	**−6.28**	**−8.88**
Autumn	—	—	—	**−2.85**	−1.8	**−2.88**	−2.93
Winter	—	—	—	−0.14	−1.25	−0.17	−0.91
Annual	**−6.53**	**−10.33**	**−4.72**	**−2.22**	**−2.35**	**−2.99**	**−3.57**

Note: Bold values denote statistical significance at the $p \leq .05$ level.

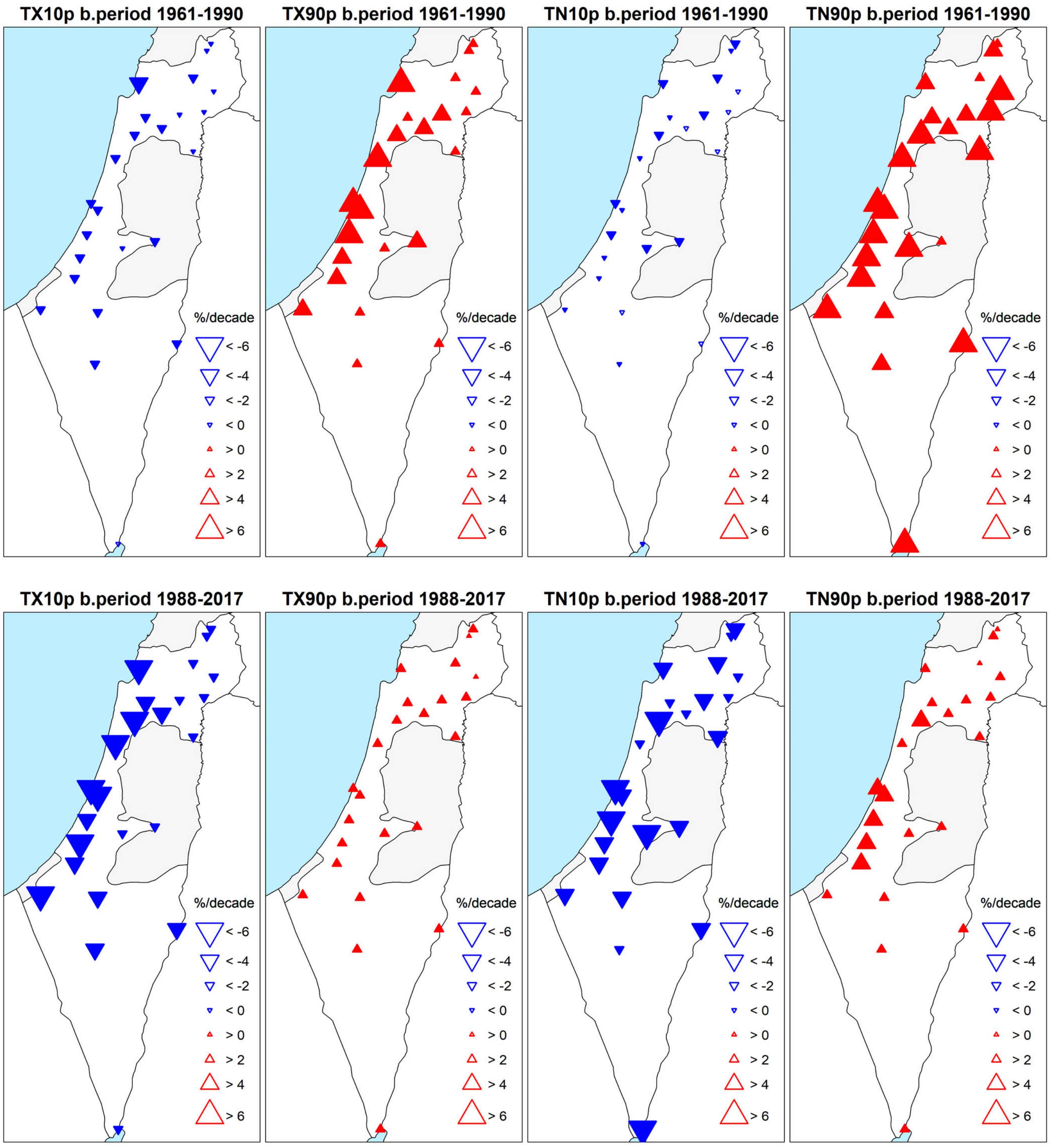

FIGURE 5 Trends in cold days (TX10p), warm days (TX90p), cold nights (TN10p) and warm nights (TN90p) for the period 1988–2017. The upper and lower panels present the trends when using 1961–1990 and 1988–2017 as the base period, respectively. Symbols as Figure 4 (units: % per decade) [Colour figure can be viewed at wileyonlinelibrary.com]

found that the trend magnitude of the cold percentile-based indices (CSDI3, TX10p, TN10p) is amplified while the trend magnitude of the warm indices (WSDI, WSDI3, TX90p, TN90p) is diminished when a warmer base period is used. These features emerge for the long-term trends and are more pronounced during the last 30 years. This result may be explained by the fact that, under conditions of continuous global warming, deriving percentiles from

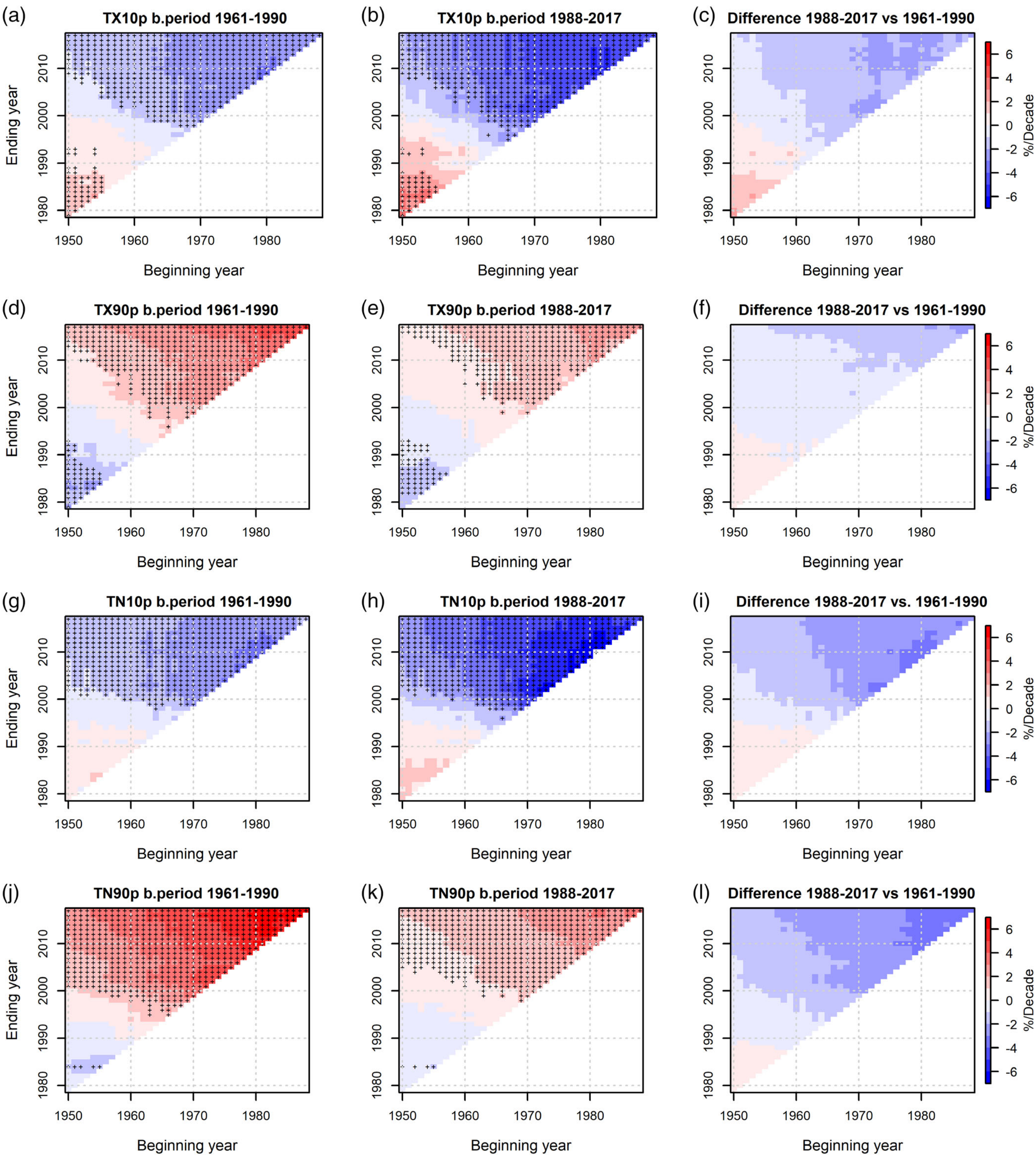

FIGURE 6 Annual trend matrix of the regional percentile-based indices: TX10p (a,b), TX90p (d,e), TN10p (g,h), and TN90p (j,k). Panels on the left-hand side use percentiles derived from the cooler base period 1961–1990. Panels on the middle use percentiles derived from the warmer base period 1988–2017. Positive (negative) trends are coloured in red (blue). "+" denotes significant trends ($p \leq .05$). Panels on the right hand shows the difference between the period when percentiles were derived from 1988–2017 (middle column) versus from 1961–1990 (left column). Units for all the panels are (% per decade) [Colour figure can be viewed at wileyonlinelibrary.com]

a distribution shifted to the right results in higher thresholds that need to be exceeded. Therefore, when the 10th percentile is derived from a recent warmer (e.g., 1988–2017) base period, the threshold (absolute) values are higher than when the 10th percentile is derived from the colder (1961–1990) base period, increasing their exceedance rate mainly in the past, thereby leading to a stronger (steeper) trend magnitude. This is unlike when the 10th percentiles were derived from 1961–1990 base period. Exceeding the thresholds derived from that distribution became quite a rare event in the past two decades. Hence, in this case the slope is much more moderate.

The opposite is true for the 90th percentile, which was derived from a warmer base period. In this case, the threshold (absolute) values again are higher than in the cooler past, thus reducing the frequency with which these high thresholds are exceeded in the past as well as these days. Hence, using a recent warmer base period may lead to the erroneous conclusion that there is only a slight increasing trend in the warm indices, which misrepresents the actual changes to global climate (unlike when using the colder base periods of 1961–1990 or even 1971–2000).

Another important finding was that estimates for the summer months (June–August) were impacted by the choice of base period much more than the winter months (December–February). This is unsurprising given that the summer in the east Mediterranean region has undergone a highly significant and substantial change (Kostopoulou and Jones, 2005; Ziv *et al.*, 2005; Shohami *et al.*, 2011; Tanarhte *et al.*, 2012; Yosef *et al.*, 2018; Yosef *et al.*, 2019). Consequently, the changes in the annual cycle of the 10th and the 90th percentiles are more pronounced in the summer than in the winter. Thus, we observed a differential change in the annual cycle, with a marked increase in summer temperatures (TX and TN) coupled with a milder increase in winter temperatures. This differential change emerged when we compared a cold base period versus a warm base period.

5 | CONCLUSIONS

The present study examined the effect of using different base periods (1961–1990 colder versus 1988–2017 warmer) on the trends calculated from the common ETCCDI percentile-based extreme temperature indices. One of the major strengths of the ETCCDI is that it enables comparisons of agreed-upon indices from comparable analyses (i.e., from analyses that use the same formulas) conducted across different parts of the world. The use of such indices, in turn, presumably facilitates seamless integration of observations obtained from different regions (calculated independently, for example, Alexander *et al.*, 2006) to produce a global picture. Although trends of "day-count" indices with fixed thresholds are impacted by the length of the period of interest, the percentile-based indices trends are susceptible to both the length of the period of interest as well as the chosen base period in the time series. Percentile-based indices are much more sensitive to the selected base period compared to alternative indices, especially in a world characterized by continuous climate change. When different base periods are used, the magnitude of the trends may change, depending on whether percentiles are derived from a relatively colder or warmer base period, given the underlying warming trend. The highest discrepancy emerges at the end of the analysed period (i.e., the warmest years). Therefore, it is important to bear in mind a striking difference in the trends calculated (two to three times or even greater) when contrasting base periods which include the last two decades versus those which do not use the normal base period 1961–1990 (e.g., Donat *et al.*, 2014; Shrestha *et al.*, 2017; Barry *et al.*, 2018; Salameh *et al.*, 2019). This is an important methodological issue for future research as well, especially in a continuously changing climate that is expected to get much warmer in coming years according to global and regional climate models.

To properly compare or integrate data from studies that use percentile-based indices either across regions or within the same region, the base period should be the same, especially in this era characterized by accelerated warming. As the current research shows, the use of different base periods when utilizing percentile-based indices runs the risk of causing researchers and policymakers alike to misestimate the magnitude of climate change.

ACKNOWLEDGEMENTS

The authors are grateful to the Climate Department of the Israel Meteorological Service for providing the data and the metadata for this study.

ORCID

Yizhak Yosef https://orcid.org/0000-0002-3010-3188

REFERENCES

Aguilar, E., Peterson, T.C., Obando, P.R., Frutos, R., Retana, J.A., Solera, M., Soley, J., García, I.G., Araujo, R.M., Santos, A.R. and Valle, V.E. (2005) Changes in precipitation and temperature extremes in Central America and northern South America, 1961–2003. *Journal of Geophysical Research: Atmospheres*, 110(D23).

Alexander, L. and Herold, N. (2015) *ClimPACTv2 Indices and Software. A Document Prepared on Behalf of the Commission for Climatology (CCl) Expert Team on Sector-Specific Climate Indices (ET-SCI)*. Sydney, Australia.

Alexander, L.V., Zhang, X., Peterson, T.C., Caesar, J., Gleason, B., Klein Tank, A.M.G., Haylock, M., Collins, D., Trewin, B., Rahimzadeh, F. and Tagipour, A. (2006) Global observed changes in daily climate extremes of temperature and precipitation. *Journal of Geophysical Research: Atmospheres*, 111 (D5).

Barry, A.A., Caesar, J., Klein Tank, A.M.G., Aguilar, E., McSweeney, C., Cyrille, A.M., Nikiema, M.P., Narcisse, K.B., Sima, F., Stafford, G. and Touray, L.M. (2018) West Africa climate extremes and climate change indices. *International Journal of Climatology*, 38, e921–e938.

Bronaugh, D. and Werner, A. (2013). zyp: Zhang + Yue-Pilon trends package. R package version, 0.10-1. http://CRAN.R-project.org/package=zyp.

Donat, M.G., Alexander, L.V., Yang, H., Durre, I., Vose, R., Dunn, R.J.H., Willett, K.M., Aguilar, E., Brunet, M., Caesar, J. and Hewitson, B. (2013) Updated analyses of temperature and precipitation extreme indices since the beginning of the twentieth century: the HadEX2 dataset. *Journal of Geophysical Research: Atmospheres*, 118(5), 2098–2118.

Donat, M.G., Peterson, T.C., Brunet, M., King, A.D., Almazroui, M., Kolli, R.K., Boucherf, D., Al-Mulla, A.Y., Nour, A.Y., Aly, A.A. and Nada, T.A.A. (2014) Changes in extreme temperature and precipitation in the Arab region: long-term trends and variability related to ENSO and NAO. *International Journal of Climatology*, 34(3), 581–592.

Frich, P., Alexander, L.V. and Della-Marta, P.M. (2002) Observed coherent changes in climatic extremes during the second half of the twentieth century. *Climate research*, 19(3), 193–212.

Intergovernmental Panel on Climate Change (IPCC). (2014) Climate Change 2014: synthesis report. In: Pachauri, R.K. and Meyer, L.A. (Eds.). *Contribution of Working Groups I, II and III to the Fifth Assessment Report of the Intergovernmental Panel on Climate Change*. Switzerland: IPCC, p. 151.

Karl, T.R., Nicholls, N. and Ghazi, A. (1999) Clivar/GCOS/WMO workshop on indices and indicators for climate extremes workshop summary. In: *Weather and Climate Extremes*. Dordrecht: Springer, pp. 3–7.

Kendall, M.G. (1955) *Rank Correlation Methods*. Charles Griffin, p. 196.

Klein Tank, A.M.G., Peterson, T.C., Quadir, D.A., Dorji, S., Zou, X., Tang, H., Santhosh, K., Joshi, U.R., Jaswal, A.K., Kolli, R.K. and Sikder, A.B. (2006) Changes in daily temperature and precipitation extremes in central and South Asia. *Journal of Geophysical Research: Atmospheres*, 111 (D16).

Klein Tank, A.M.G., Zwiers, F.W. and Zhang, X. (2009). *Guidelines on analysis of extremes in a changing climate in support of informed decisions for adaptation. Climate data and monitoring, WCDMP-No. 72, WMO-TD No.1500*. Geneva, Switzerland.

Kostopoulou, E. and Jones, P.D. (2005) Assessment of climate extremes in the eastern Mediterranean. *Meteorology and Atmospheric Physics*, 89(1–4), 69–85.

Mann, H.B. (1945) Non-parametric tests against trend. *Econometrica*, 13, 245–259.

Peterson, T., Folland, C., Gruza, G., Hogg, W., Mokssit, A. and Plummer, N. (2001). *Report on the Activities of the Working Group on Climate Change Detection and Related Rapporteurs 1998–2001*. WMO, Rep. WCDMP-47, WMO-TD 1071, Geneve, Switzerland, 143 pp.

Salameh, A.A., Gámiz-Fortis, S.R., Castro-Díez, Y., Abu Hammad, A. and Esteban-Parra, M.J. (2019) Spatio-temporal analysis for extreme temperature indices over Levant region. *International Journal of Climatology*, 39(15), 5556–5582. https://doi.org/10.1002/joc.6171.

Sen, P.K. (1968) Estimates of the regression coefficient based on Kendall's tau. *Journal of the American Statistical Association*, 63, 1379–1389.

Shohami, D., Dayan, U. and Morin, E. (2011) Warming and drying of the eastern Mediterranean: additional evidence from trend analysis. *Journal of Geophysical Research: Atmospheres*, 116(D22).

Shrestha, A.B., Bajracharya, S.R., Sharma, A.R., Duo, C. and Kulkarni, A. (2017) Observed trends and changes in daily temperature and precipitation extremes over the Koshi river basin 1975–2010. *International Journal of Climatology*, 37(2), 1066–1083.

Tanarhte, M., Hadjinicolaou, P. and Lelieveld, J. (2012) Intercomparison of temperature and precipitation data sets based on observations in the Mediterranean and the Middle East. *Journal of Geophysical Research: Atmospheres*, 117(D12).

Vincent, L.A. and Mekis, E. (2006) Changes in daily and extreme temperature and precipitation indices for Canada over the twentieth century. *Atmosphere-Ocean*, 44(2), 177–193.

Wang, X.L. and Swail, V.R. (2001) Changes of extreme wave heights in northern hemisphere oceans and related atmospheric circulation regimes. *Journal of Climate*, 14, 2204–2220.

World Meteorological Organization. (2017). *WMO guidelines on the calculation of climate normal, WMO-No. 1203*. Geneva, Switzerland.

Yosef, Y., Aguilar, E. and Alpert, P. (2018) Detecting and adjusting artificial biases of long-term temperature records in Israel. *International Journal of Climatology*, 38(8), 3273–3289. https://doi.org/10.1002/joc.5500.

Yosef, Y., Aguilar, E. and Alpert, P. (2019) Changes in extreme temperature and precipitation indices: using an innovative daily homogenized database in Israel. *International Journal of Climatology*, 39, 1–24. https://doi.org/10.1002/joc.6125.

Zhang, X., Aguilar, E., Sensoy, S., Melkonyan, H., Tagiyeva, U., Ahmed, N., Kutaladze, N., Rahimzadeh, F., Taghipour, A., Hantosh, T.H. and Alpert, P. (2005a) Trends in Middle East climate extreme indices from 1950 to 2003. *Journal of Geophysical Research: Atmospheres*, 110(D22).

Zhang, X., Hegerl, G., Zwiers, F.W. and Kenyon, J. (2005b) Avoiding inhomogeneity in percentile-based indices of temperature extremes. *Journal of Climate*, 18(11), 1641–1651.

Zhang, X., Alexander, L., Hegerl, G.C., Jones, P., Tank, A.K., Peterson, T.C., Trewin, B. and Zwiers, F.W. (2011) Indices for monitoring changes in extremes based on daily temperature and precipitation data. *Wiley Interdisciplinary Reviews: Climate Change*, 2(6), 851–870.

Zhang, X., Hogg, W.D. and Bonsal, B.R. (2001) A cautionary note on the use of seasonally varying thresholds to assess temperature extremes. *Climatic Change*, 50(4), 505–507.

Zhang, X., Vincent, L.A., Hogg, W.D. and Niitsoo, A. (2000) Temperature and precipitation trends in Canada during the 20th century. *Atmosphere-Ocean*, 38(3), 395–429.

Ziv, B., Saaroni, H., Baharad, A., Yekutieli, D. and Alpert, P. (2005) Indications for aggravation in summer heat conditions over the Mediterranean Basin. *Geophysical Research Letters*, 32(12).

How to cite this article: Yosef Y, Aguilar E, Alpert P. Is it possible to fit extreme climate change indices together seamlessly in the era of accelerated warming? *Int J Climatol*. 2020;1–12. https://doi.org/10.1002/joc.6740